Springer

KSME

Journal of Mechanical Science and Technology 24 (12) (2010) 2519~2527
www.springerlink.com/content/1738-494x
DOI 10.1007/s12206-010-0918-y

Thermal buckling analysis of cross-ply laminated rectangular plates under nonuniform temperature distribution: A differential quadrature approach †

M. Mansour Mohieddin Ghomshei* and Amin Mahmoudi

Department of Mechanical Engineering, Islamic Azad University-Karaj Branch, Karaj, Alborz, 31485-313, I.R. Iran

(Manuscript Received March 29, 2010; Revised August 31, 2010; Accepted August 31, 2010)

Abstract

Differential quadrature method (DQM) is implemented for analyzing the thermal buckling behavior of the symmetric cross-ply laminated rectangular thin plates subjected to uniform and/or non-uniform temperature fields. The approach includes two steps: (1) solving the problem of in-plane thermo-elasticity to obtain the in-plane force resultants and (2) solving the buckling problem under the force distribution obtained in the previous step. Solution procedures are numerically performed by discretizing the governing differential equations and boundary conditions using DQM method. Applying the developed DQ formulation, the buckling loads are obtained for several sample plates. The numerical results compared well with those available in the literature as well as those obtained by ABAQUS. Parametric studies are conducted to investigate the influence of some important parameters including the plate aspect ratio, cross-ply ratio, and stiffness ratio on the critical temperature and mode shape of buckling.

Keywords: Thermal buckling; DQM; Cross-ply laminate; Non-uniform thermal load; Laminated plate

1. Introduction

Thermal buckling is a crucial failure mode in plates and shells. When geometrically perfect plates restrained from in-plane expansion are slowly heated, they generally develop compressive stresses and then buckle at a specific temperature. Attention was first given to thermal buckling problem during the onset of the jet age, when aircraft and missile structural elements, such as plates and shells became exposed to high temperatures inherent to supersonic flight. Fiber-reinforced composite laminates have important structural applications in aircraft and space vehicles and other weight-sensitive applications, These materials are usually subjected to non-uniform temperature distributions due to aerodynamic and solar radiation heating. In this respect, the analysis of thermal buckling due to non-uniform thermal load is of special interest.

Thangaratnam and Ramachandran [1] studied thermal buckling behavior of composite laminated plates subjected to a uniform temperature distribution on simple edge supports. Chen et al. [2-4] used the finite element method to study the problems of thermal buckling and postbuckling behavior of composite laminated plates, taking into account the effect of transverse normal strain. Chen et al. [5] also analyzed the thermal buckling behavior of composite laminated plates subjected to non-uniform temperature fields using the finite element method, wherein the effect of shear deformation and rotary inertia was accounted for using thermal-elastic Mindlin plate theory. Implementing the equivalent mechanical loading concept, Jones [6] developed solutions for unidirectional and symmetric cross-ply laminated fiber-reinforced composite rectangular plates and uniform heating throughout the plate volume that are uniaxially restrained in their plane on two of the four edges, but have no rotational restraint on any edge.

In this research, the problem of thermal buckling behavior of thin unidirectional and symmetric cross-ply laminated fiber-reinforced composite rectangular plates under uniform or non-uniform temperature field is studied by implementing the differential quadrature method (DQM). Parametric studies are conducted to investigate the influence of various important parameters, including plate aspect ratio, cross-ply ratio, stiffness ratio, and boundary conditions on the critical thermal load and mode shape of buckling.

2. Governing equations

Consider a thin rectangular composite plate with length *a,* width *b*, and thickness *t*, which has a symmetric cross-ply laminated structure (so-called laminate), as shown in Fig. 1. The plate is subjected to a non-uniformly distributed temperature change $T(x,y)$, which is an arbitrary function of in-plane

† This paper was recommended for publication in revised form by Associate Editor Maenghyo Cho

* Corresponding author. Tel.: +98261-4418143-9, Fax.: +98261-4418156
E-mail address: ghomshei@kiau.ac.ir

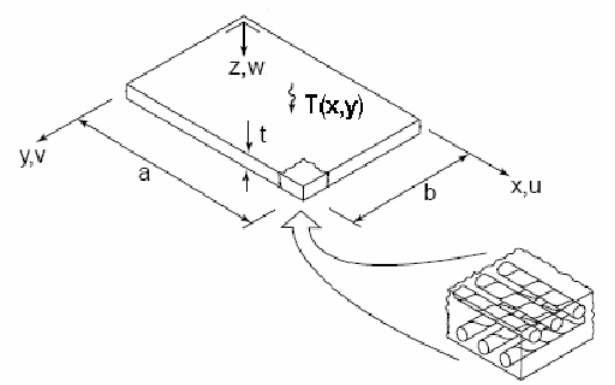

Fig. 1. A cross-ply laminated rectangular plate subjected to a nonuniformely distributed thermal load.

coordinates *x, y*, but is constant throughout the plate thickness (*z* coordinate). We assume that T (x,y) is expressed as $T_0 \times \overline{T}(x,y)$, where T_0 is the absolute maximum or minimum value of the function T (x,y), which can be considered the index value of the temperature distribution. Thermal load can cause the plate to buckle due to thermal stresses. To determine the critical values of the temperature distribution index T_0 at the onset of buckling, we perform two main steps: (1) solving the problem of plane elasticity to obtain pre-buckling in-plane force resultants as functions of the thermal load index T_0, and (2) solving the buckling problem under the force distribution obtained in the first step, which leads to the value of the critical temperature index T_0. Solution procedures are numerically performed by discretizing the governing differential equations and boundary conditions using differential quadrature method (DQM), as will be discussed in section 3.

2.1 Kinematics and constitutive relations

The classical laminated plate theory is adopted, because of the thin plate assumption. Thus, the nonzero strain components in terms of midplane strains and curvatures are given by

$$\begin{aligned}\varepsilon_x &= \varepsilon_x^0 + z\kappa_x,\\ \varepsilon_y &= \varepsilon_y^0 + z\kappa_y,\\ \gamma_{xy} &= \gamma_{xy}^0 - 2z\kappa_{xy}\end{aligned} \tag{1}$$

where $\varepsilon_x^0, \varepsilon_y^0, \gamma_{xy}^0$ and $\kappa_x, \kappa_y, \kappa_{xy}$ are midplane strains and curvatures, respectively. These values are related to the displacement field as [7]

$$\begin{aligned}&\varepsilon_x^0 = u_{,x} + \frac{1}{2}w_{,x}^2, \quad \kappa_x = -w_{,xx},\\ &\varepsilon_y^0 = v_{,y} + \frac{1}{2}w_{,y}^2, \quad \kappa_y = -w_{,yy},\\ &\gamma_{xy}^0 = (u_{,y} + v_{,x}) + w_{,x}w_{,y}, \quad \kappa_{xy} = w_{,xy}\end{aligned} \tag{2}$$

where *u*, *v*, and *w* are the displacements along *x*, *y*, and *z* axes, respectively. Subscripts following a comma stand for partial differentiations. The second-order terms in the midplane strain expressions are accounted for, because of the large deflection occurrence in the buckling phenomenon.

Considering thermal effects, the lamina stress-strain relations expressed for the k^{th} ply are given as [8]

$$\{\sigma\}_k = \left[\overline{Q_{ij}}\right]_k (\{\varepsilon^0\} + z\{\kappa\} - \{\alpha\}_k \Delta T)$$
(k= ply number) (3)

in that, $\{\sigma\}_k = \{\sigma_x, \sigma_y, \tau_{xy}\}_k^T$ is a vector of stress components in the k^{th} ply. Multiplying the two sides of the recent equation by 1 and *z*, and then integrating them over the laminate thickness, the laminate constitutive equations are obtained as [8]

$$\begin{Bmatrix} N \\ M \end{Bmatrix} = \begin{bmatrix} A & B \\ B & D \end{bmatrix} \begin{Bmatrix} \varepsilon^0 \\ \kappa \end{Bmatrix} - \begin{Bmatrix} N^T \\ M^T \end{Bmatrix} \tag{4}$$

where $\{N\} = \{N_x, N_y, N_{xy}\}^T$ and $\{M\} = \{M_x, M_y, M_{xy}\}^T$ are vectors of the resultant mechanical in-plane force and moment components, and A, B and D are respectively extensional, coupling and bending stiffness matrices determined by the following summations [8]

$$\begin{aligned}[A] &= \sum_{k=1}^{n} [\bar{Q}]_k (z_k - z_{k-1}),\\ [B] &= \frac{1}{2}\sum_{k=1}^{n} [\bar{Q}]_k (z_k^2 - z_{k-1}^2),\\ [D] &= \frac{1}{3}\sum_{k=1}^{n} [\bar{Q}]_k (z_k^3 - z_{k-1}^3)\end{aligned} \tag{5}$$

where $[\bar{Q}]_k$ is the reduced transformed lamina stiffness matrix for the k^{th} ply, which can be calculated for the plies having 0° or 90° fiber directions by [8]

$$\left[\bar{Q}\right]_{0^\circ} = \begin{bmatrix} \dfrac{E_1}{1-\nu_{12}\nu_{21}} & \dfrac{\nu_{12}E_2}{1-\nu_{12}\nu_{21}} & 0 \\ & \dfrac{E_2}{1-\nu_{12}\nu_{21}} & 0 \\ SYMM. & & G_{12} \end{bmatrix},$$

$$\left[\bar{Q}\right]_{90^0} = \begin{bmatrix} \dfrac{E_2}{1-\nu_{12}\nu_{21}} & \dfrac{\nu_{12}E_2}{1-\nu_{12}\nu_{21}} & 0 \\ & \dfrac{E_1}{1-\nu_{12}\nu_{21}} & 0 \\ SYMM. & & G_{12} \end{bmatrix} \tag{6}$$

The thermal force and moment vectors $\{N^T\}$, $\{M^T\}$ in Eq. (4), are determined by [8]

$$[N]^T = \begin{bmatrix} N_x^T \\ N_Y^T \\ N_{XY}^T \end{bmatrix} = \sum_{k=1}^{n} \int_{z_k}^{z_{k-1}} \left[\overline{Q_{ij}^k}\right] \begin{bmatrix} \alpha_x \\ \alpha_y \\ 2\alpha_{xy} \end{bmatrix} \Delta T \, dz \,,$$

$$[M]^T = \begin{bmatrix} M_x^T \\ M_Y^T \\ M_{XY}^T \end{bmatrix} = \sum_{k=1}^{n} \int_{z_k}^{z_{k-1}} \left[\overline{Q_{ij}^k}\right] \begin{bmatrix} \alpha_x \\ \alpha_y \\ 2\alpha_{xy} \end{bmatrix} \Delta T\, z\, dz \,. \tag{7}$$

Regarding the symmetric laminate assumption, the coupling stiffness matrix and the thermal moment vector vanish, (i.e. $[B]=0$, M^T=0). After simplifying, we solve Eq. (4) for ε_0, κ, and obtain

$$\begin{Bmatrix} \varepsilon^0 \\ \kappa \end{Bmatrix} = \begin{bmatrix} A & 0 \\ 0 & D \end{bmatrix}^{-1} \left(\begin{Bmatrix} N \\ M \end{Bmatrix} + \begin{Bmatrix} N^T \\ 0 \end{Bmatrix} \right). \tag{8}$$

2.2 Pre-buckling force state

The thermal stresses caused by non-uniform temperature distribution generate non-uniformly distributed membrane force resultants in the plate. All mechanical and thermal moments and consequently curvatures vanish (M=M_T=κ=0) in pre-buckling, thus the membrane forces can be determined by solving the plane elasticity problem. The compatibility equation in terms of midplane strains in a plane stress state is given by [9]

$$\frac{\partial^2 \varepsilon_x^0}{\partial y^2} + \frac{\partial^2 \varepsilon_y^0}{\partial x^2} = \frac{\partial^2 \gamma_{xy}^0}{\partial x \partial y} \tag{9}$$

To obtain midplane strains in terms of membrane forces, Eq. (8) can be simplified and rewritten as

$$\{\varepsilon^0\} = [A]^{-1} \left(\{N\} + \{N^T\} \right) \,. \tag{10}$$

On the other hand, we have the differential form of force equilibrium equations for a laminated plate:

$$N_{x,x} + N_{xy,y} = 0 \,, \quad N_{xy,x} + N_{y,y} = 0 \,. \tag{11}$$

We substitute Eq. (10) to Eq. (9), then replace the derivatives of N_y, N_{xy} with the derivatives of N_x using Eq. (11). After non-dimensionalization, we achieve the following partial differential equation for N_x:

$$\begin{aligned} &A'_{22}\left(\frac{\partial^4 N_X}{\partial X^4}\right) + \left(2A'_{12} + A'_{66}\right)\beta^2 \left(\frac{\partial^4 N_X}{\partial X^2 \partial Y^2}\right) + A'_{11}\beta^4 \left(\frac{\partial^4 N_X}{\partial Y^4}\right) = \\ &-\left\{ A'_{11}\beta^4 \left(\frac{\partial^4 N_X^T}{\partial Y^4}\right) + A'_{12}\beta^2 \left(\beta^2 \frac{\partial^4 N_Y^T}{\partial Y^4} + \frac{\partial^4 N_X^T}{\partial X^2 \partial Y^2} \right) \right\} \\ &-\left\{ A'_{22}\beta^2 \left(\frac{\partial^4 N_Y^T}{\partial X^2 \partial Y^2}\right) - A'_{66}\beta^3 \left(\frac{\partial N_{XY}^T}{\partial X \partial Y^3}\right) \right\} \end{aligned} \tag{12}$$

where A'_{ij} are the entries of $[A']$= $[A]^{-1}$; X and Y are non-dimensional in-plane coordinates defined as $X = x/a$, $Y = y/b$; and $\beta = a/b$ is the plate aspect ratio. By solving Eq. (12) with its boundary conditions, the distribution of in-plane force N_x is obtained. By applying Eq. (11), the two other membrane forces N_y and $N_{xy,}$ which are functions of X, Y with a linear dependence to the thermal load index $T_{0,}$ are determined.

2.3 Thermal buckling behavior

Consider the buckling of the thin laminated plate shown in Fig. 1. We use the principle of minimum total potential energy to derive equilibrium and stability equations of the laminated plate under non-uniform thermal loading. The total potential energy of such a plate can be determined by [8]

$$\Pi = \frac{1}{2} \iiint \left[\sigma\right]^T \left(\{\varepsilon\} - T\{\alpha\} \right) dx dy dz \,. \tag{13}$$

By substituting from Eq. (3) into the right-hand side of the recent equation, performing the integration over the thickness coordinate z, then using Eqs. (5) and (7), we obtain

$$\begin{aligned} \Pi = \frac{1}{2} \int_0^b \int_0^a \Big[&\left(\{\varepsilon^0\}^T [A] \{\varepsilon^0\} + 2\{\varepsilon^0\}^T [B] \{\kappa\} - 2\{\varepsilon^0\}^T \{N^T\} + \right. \\ &\left. \{\kappa\}^T [D] \{\kappa\} \right) - \left(2\{\kappa\}^T \{M^T\} - \int_{-h/2}^{h/2} \{\alpha\}^T [\bar{Q}] \{\alpha\} T^2 dz \right) \Big] dx dy. \end{aligned} \tag{14}$$

By substituting from Eq. (8) into the right-hand side of the recent equation, then implementing the Euler-Lagrange equations on the integrant of the final expression obtained for Π, the plate equilibrium equations are derived as follows:

$$\begin{aligned} &N_{x,x} + N_{xy,y} = 0 \,, \\ &N_{xy,x} + N_{y,y} = 0 \,, \\ &M_{x,xx} + 2M_{xy,xy} + M_{y,yy} + N_x W_{,xx} + 2N_{xy} W_{,xy} + N_y W_{,yy} = 0 \end{aligned} \tag{15}$$

In Eq. (15), the first two equations are the force equilibrium equations as mentioned in the previous section. Expressing the moments M_x, M_y and M_{xy} in terms of derivatives of w in the third equation, we obtain the governing differential equation of lateral deflection and buckling behavior in the laminated plate, which can be expressed in non-dimensional form as

$$\begin{aligned} &D_{11} W_{,XXXX} + 2\left(D_{12} + 2D_{66}\right)\beta^2 W_{,XXYY} + D_{22}\beta^4 W_{,YYYY} = \\ &a^2 \left(N_X W_{,XX} + 2\beta N_{XY} W_{,XY} + \beta^2 N_Y W_{,YY} \right) \\ &\text{in that, } W = w/h \,. \end{aligned} \tag{16}$$

3. Differential quadrature formulation

DQM which was introduced by Bellman and Casti (as reported in Ref. [10]) is a numerical technique for solving boundary value problems. DQM needs much less computations than other numerical methods such as FEM. DQM is briefly reviewed in this section.

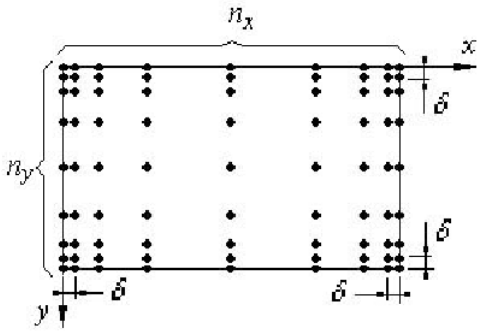

Fig. 2. Sketch of a rectangular plate with ordinary grid points and δ-points near the boundary points.

3.1 Review of the quadrature rule

In DQM the derivative of a function with respect to a space variable can be approximated by a weighted linear combination of the function values at some intermediate points in the domain of that variable. A multiple derivative of a function $f(x,y)$ of order r with respect to x, and of order s with respect to y ($r, s \geq 0$), at an intermediate discrete point (x_i, y_j) can be approximated by the weighted linear sum of the function values as

$$\frac{\partial^{r+s} f(x_i,y_j)}{\partial x^r \partial y^s} = \sum_{k=1}^{n_x} C_{ik}^{x(r)} \sum_{l=1}^{n_y} C_{jl}^{y(s)} f(x_k,y_l) \ , \quad i=1,...,n_x \ , j=1,...,n_y \tag{17}$$

where $C_{ik}^{x(r)}$ and $C_{ik}^{x(r)}$ are entries of the weighting coefficient matrices of partial derivatives $\partial^r f/\partial x^r$, $\partial^s f/\partial y^s$ respectively, which can be computed by

$$[C^{x(r)}] = [C^{x(1)}]^r \ , \ [C^{y(s)}] = [C^{y(1)}]^s \tag{18}$$

where $[C^{x(1)}]$, $[C^{y(1)}]$ are the weighting coefficient matrices for the first-order partial derivatives $\partial/\partial x$, $\partial/\partial y$ respectively. Adopting the generalized differential quadrature method (GDQM), which assumes Lagrange interpolation function as the test function, the weighting coefficients are computed by [10]

$$C_{ij}^{(1)} = \frac{1}{(x_i - x_j)} \frac{\prod_{k=1,k\neq i}^{N} (x_i - x_k)}{\prod_{k=1,k\neq j}^{N} (x_j - x_k)} \ , \ i,j=1, \ ..., \ n, \ i \neq j. \tag{19}$$

For selecting grid points, the procedure of Shu and Richards is adopted [10]:

$$x_i = a\left[\frac{1}{2}\left[1 - \cos\left(\frac{i-1}{N-1}\pi\right)\right]\right]. \tag{20}$$

As the partial differential Eqs. (12) and (16) are of the fourth-order with respect to both x and y coordinates, we have to satisfy two boundary conditions in each edge of the plate. To satisfy the two sets of boundary conditions in each edge, we utilize the δ-point technique. According to the technique, an additional set of grid points should be included in the vicinity of the boundary grid points at a very small distance of order $\delta=10^{-5}$ to boundary points, as shown in Fig. 2. One of the boundary conditions is applied to the boundary grid points, whereas the other can be applied to the δ-points.

3.2 Discretization by DQM

By implementing the GDQM for discretizing the plane elasticity problem, Eq. (12), and noting that $N_{XY}^T = 0$ for cross-ply laminates, the discrete form of the equation becomes

$$\begin{aligned} &A'_{22}[C^{X(4)}][N_X] + (2A'_{12} + A'_{66})\beta^2[C^{X(2)}][N_X][C^{Y(2)}]^T \\ &+ A'_{11}\beta^4[N_X][C^{Y(4)}] = -\{ A'_{11}\beta^4[N_X^T][C^{Y(4)}] + \\ &A'_{12}\beta^4[N_Y^T][C^{Y(4)}] + A'_{12}\beta^2[C^{X(2)}][N_X^T][C^{Y(2)}]^T + \\ &A'_{22}\beta^2[C^{X(2)}][N_Y^T][C^{Y(2)}]^T\} \end{aligned} \tag{21}$$

where the grid point variable $[N_X]$ is a matrix of $n_x \times n_y$ dimensions. This equation should be expanded in a way that the entries of the matrix $[N_X]$ are rearranged in a column vector of $(n_x \times n_y) \times 1$ dimensions, namely,

$$\begin{aligned} &\left(A'_{22}[C^{X(4)}]_{\exp} + (2A'_{12} + A'_{66})\beta^2[C^{X(2)}]_{\exp}[C^{Y(2)}]_{\exp} + \right. \\ &\left. A'_{11}\beta^4[C^{Y(4)}]_{\exp}\right) \times \{N_X\} = -\left[\left(A'_{11}\beta^4[C^{Y(4)}]_{\exp} + \right. \right. \\ &\left. A'_{12}\beta^2[C^{X(2)}]_{\exp}[C^{Y(2)}]_{\exp}\right)\{N_X^T\} + \\ &\left. \left(A'_{12}\beta^4[C^{Y(4)}]_{\exp} + A'_{22}\beta^2[C^{X(2)}]_{\exp}[C^{Y(2)}]_{\exp}\right)\{N_Y^T\}\right] \end{aligned} \tag{22}$$

which may be expressed in a compact form as

$$\begin{bmatrix} Coefficient \\ Matrix \end{bmatrix}_{n_x n_y \times n_x n_y} \{N_X\}_{n_x n_y \times 1} = T_{\circ cr} \begin{Bmatrix} Force \\ Vector \end{Bmatrix}_{n_x n_y \times 1} \tag{23}$$

where T_{0cr} is the critical temperature index. After imposition of the discrete form of the boundary conditions, the recent equation can be solved for the vector of nodal values of N_X. Then, the two other mechanical force components N_Y, N_{XY} are obtained by the following equations.

$$\begin{aligned} &\{N_Y\} = [C^{Y(2)}]_{\exp}^{-1}[C^{X(2)}]_{\exp}\{N_X\} \ , \\ &\{N_{XY}\} = \left([C^{X(1)}]_{\exp}[C^{Y(1)}]_{\exp}\right)^{-1}[C^{X(2)}]_{\exp}\{N_X\}. \end{aligned} \tag{24}$$

Following GDQM, the governing equation of the plate buckling behavior, Eq. (16), can also be discretized, as stated below directly in the expanded form

$$\begin{aligned} &\left(D_{11}[C^{X(4)}]_{\exp} + 2(D_{12} + 2D_{66})\beta^2[C^{X(2)}]_{\exp}[C^{Y(2)}]_{\exp} + \right. \\ &\left. \beta^4 D_{22}[C^{Y(4)}]_{\exp}\right) \times \{W\} = a^2 \left(\{N_X\}[C^{X(2)}]_{\exp} + \right. \\ &\left. 2\{N_{XY}\}\beta[C^{X(1)}]_{\exp}[C^{Y(1)}]_{\exp} + \{N_Y\}\beta^2[C^{Y(2)}]_{\exp}\right)\{W\} \end{aligned} \tag{25}$$

where the pre-buckling mechanical forces N_X , N_Y, and N_{XY} are previously determined by Eqs. (23) and (24), which are linearly dependent on the critical temperature index T_{0cr}. Thus, Eq. (25) can be rewritten in the following compact form:

$$\left[A \right]\left\{ W \right\} = \lambda \left[B \right]\left\{ W \right\} \tag{26}$$

where [A] is sum of the matrices in the parentheses of the left side of Eq. (25), and [B] is that of the right side of Eq. (25), in which $\lambda = T_{0cr}$ has been factorized. By imposing the discrete form of the boundary conditions on the recent equation, and then rearranging it in a way that all entries corresponding to the boundary grid points are placed at the top of the transverse displacement vector $\{W\}$, we have

$$\left[\begin{array}{c|c} A_{bb} & A_{bi} \\ \hline A_{ib} & A_{ii} \end{array} \right] \left\{ \begin{array}{c} W_b \\ \hline W_i \end{array} \right\} = \lambda \left[\begin{array}{c|c} 0 & 0 \\ \hline B_{ib} & B_{ii} \end{array} \right] \left\{ \begin{array}{c} W_b \\ \hline W_i \end{array} \right\}. \tag{27}$$

The boundary grid points displacement vector, $\{W_b\}$, can easily be eliminated from the above matrix equation, leading to the following homogenous system of algebraic equations for W_i

$$\left[A^* \right]\{W_i\} = \lambda \left[B^* \right]\{W_i\} \tag{28}$$

where

$$\begin{aligned} \left[A^* \right] &= \left(\left[A_{ij} \right] - \left[A_{ib} \right]\left[A_{bb} \right]^{-1}\left[A_{bi} \right] \right), \\ \left[B^* \right] &= \left(\left[B_{ij} \right] - \left[B_{ib} \right]\left[A_{bb} \right]^{-1}\left[A_{bi} \right] \right). \end{aligned} \tag{29}$$

The necessary and sufficient condition for Eq. (28) to have a non-trivial solution is

$$\left| \left[A^* \right] - \lambda \left[B^* \right] \right| = 0 . \tag{30}$$

By solving the above characteristic equation for $\lambda = T_{0cr}$, we achieve the critical values of the temperature distribution index. Then, by substituting these values into Eq. (28), we obtain the buckling mode shapes.

4. Numerical results and discussion

In this section, the numerical results obtained by the developed DQ formulation are presented. First, the convergence of the numerical solution method is investigated. The validation of the DQ model is justified by comparing the numerical results obtained for some sample problems with those reported in published papers or those obtained by a finite element analysis performed in ABAQUS. Finally, the effects of various important parameters on the critical thermal load and mode shape of buckling are studied using the present numerical solution.

Table 1. Composite laminae properties.

Material	E_1 (Gpa)	E_2 (Gpa)	ν_{12} (−)	G_{12} (Gpa)	α_1 (10^{-6}/℃)	α_2 (10^{-6}/℃)
(GY-70-HYE1534) High-modulus graphite/epoxy	90	6.9	0.25	4.8	-1.04	29.7
(AS-3501) High-strength graphite/epoxy	128	11	0.25	4.5	0.45	27.4

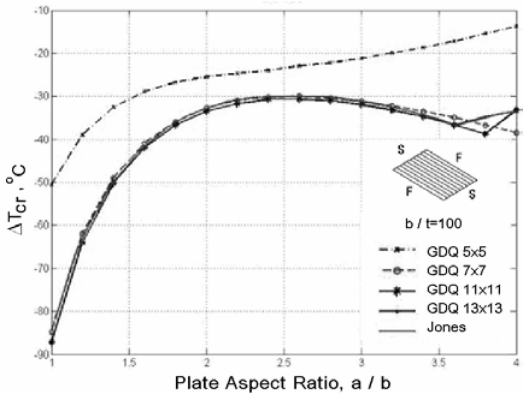

Fig. 3. Thermal buckling of a unidirectionally laminated composite plate with fiber orientation parallel to the restraint direction. Convergence of the GDQM as the number of the grid points increases.

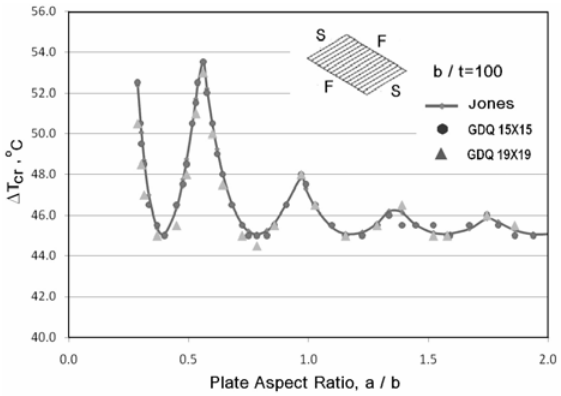

Fig. 4. Thermal buckling of a unidirectionally laminated composite plate with fiber orientation normal to the restraint direction. Comparison between the present GDQM solution and that of Ref. [6].

4.1 Convergence and validation of present formulation

To study the convergence of the presented differential quadrature formulation, a MATLAB program is prepared, and for some cases, executed several times with different grid points. The results are then compared to those available in literature.

4.1.1 Orthotropic plate under uniform thermal load

In this section, the thermal buckling load of a unidirection-

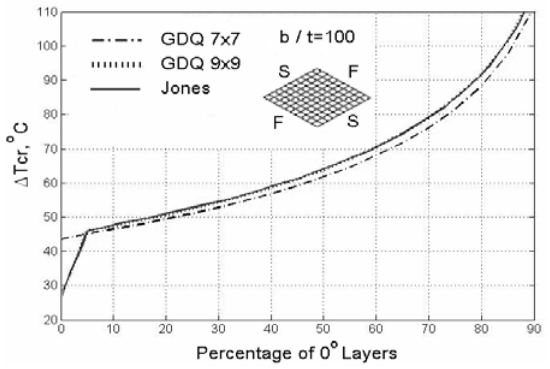

Fig. 5. Thermal buckling of a [0°/90°/0°] laminated plate of a/b=1, b/t=100. Present GDQM solution and that of Ref [6].

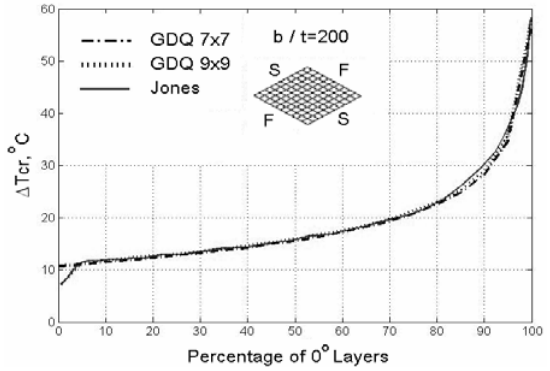

Fig. 6. Thermal buckling of a [0°/90°/0°] laminated plate of a/b=1, b/t=200. Present GDQM solution and that of Ref [6].

ally laminated fibrous composite plate is computed using a set of different numbers of grid points. The numerical results are then compared with those of Ref. [6]. The laminate is fabricated from high-modulus graphite-epoxy laminae (GY-70-HYE1534), whose properties are listed in Table 1. The two edges of the plate normal to x axis are simply supported, whereas the two others are free (briefly indicated as SSFF). The plate is subjected to a uniform temperature change $T(x,y)=\Delta T$. Fibers are oriented parallel to the restraint direction (along x axis), with width to thickness ratio of b/t=100. The present solution for ΔT_{cr} versus aspect ratio, a/b, is shown in Fig. 3, together with the solution reported by Jonse [6]. Based on the figure, for a grid of 7×7 accuracy points or more, the results of GDQ have very good correspondence with those of Ref. [6]. Note that a plate made of high-modulus graphite-epoxy with its negative α_1 must be cooled to buckle, not heated.

The solution for a case of a unidirectionally laminated composite plate same as that described in the previous paragraph, but here with fiber orientation normal to the restraint direction (*i.e.*, along y axis), are presented in Fig. 4. The results are obtained with two different sets of grid points, (*i.e.*, 15×15 and 19×19) which show good agreements with solution reported by Jones [6]. However, the latter set shows better agreement especially at higher mode shapes of buckling. Therefore, to

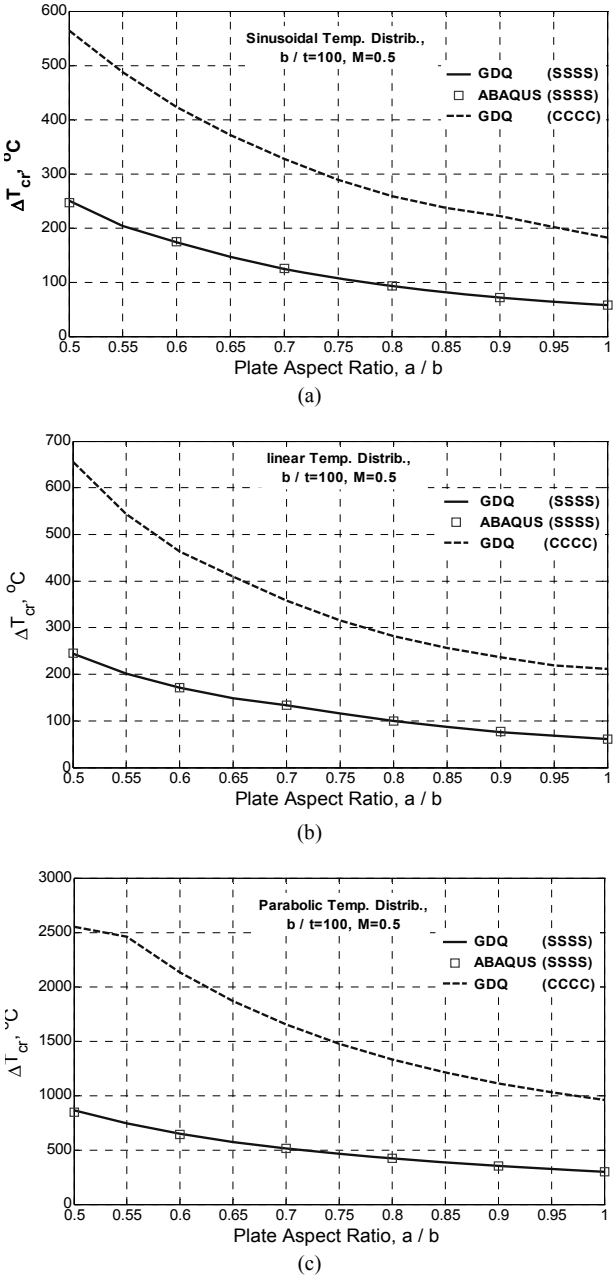

Fig. 7. ΔT_{cr} versus aspect ratio, for a symmetric [0°/90°/0°] laminated plate of b/t=100, M=0.5, simply supported and fully clamped under (a) linear, (b) paraboloidal, and (c) sinusoidal thermal load.

achieve sufficiently accurate results, a greater number of grid points should be selected as the plate buckles in higher mode numbers. Also, it can be deduced that the plate has been buckled in higher mode shapes for this case than the previous one as the aspect ratio varies from 0.25 to 2.0. Variable ΔT_{cr} is not highly dependent on a/b and approaches its constant minimum value at relatively low a/b, which is in contrast with the behavior of the previous case.

4.1.2 Cross-ply laminated plate under uniform thermal load

In this section, the thermal buckling loads for a case of a

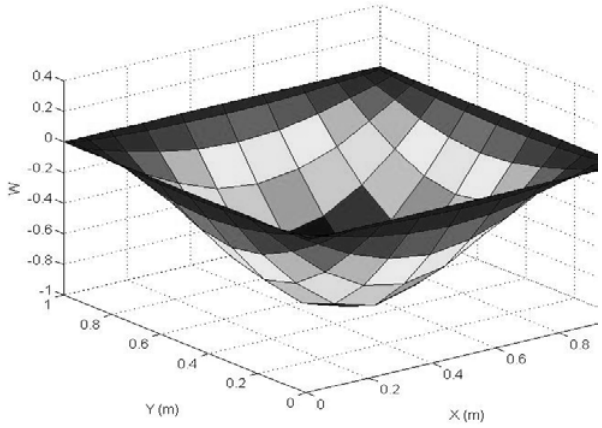

(a)

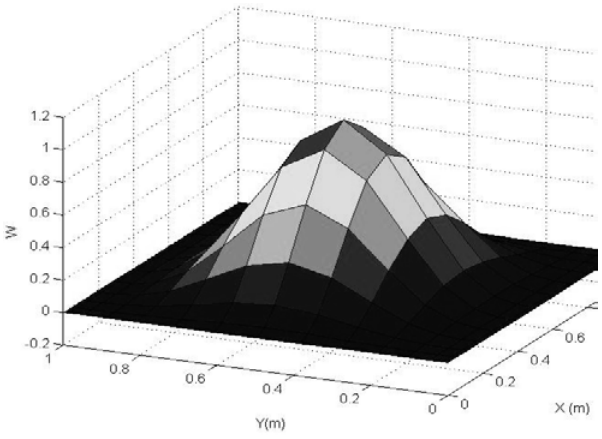

(b)

Fig. 8. Thermal buckling mode shapes for a symmetric [0°/90°/0°] laminated plate of a/b=1, b/t=100 and M=0.5, under a sinusoidal thermal load for edge supporting (a) SSSS, and (b) CCCC.

symmetric cross-ply laminated plate, with stacking sequence [0°/ 90°/ 0°], is computed using grid points of 7×7 and 9×9. Then, the numerical results are compared to those of Ref. [6]. The plate has a square shape (*i.e.* a/b=1) and the edge supports are arranged as SSFF, with two simply supported edges normal to x axis. The plate is under a uniform temperature change ΔT similar to the previous cases, however, the assumed material for the plate is a high-strength graphite-epoxy laminae (AS-3501), whose properties are listed in Table 1. The results obtained by the present DQ model for ΔT_{cr} versus the percentage of 0° layers in laminate thickness for two different width to thickness ratios, (*i.e.* b/t=100 and b/t=200) are depicted in Figs. 5 and 6 respectively. For a grid with 9×9 accuracy points, the results of GDQM have an excellent correspondence with those reported by Jonse [6].

4.1.3 A laminated plate under different nonuniform thermal loads

Thermal buckling of a symmetric cross-ply laminated plate of stacking sequence [0°/90°/0°] under three different thermal load distributions (*i.e.*, a linear, paraboloidal, and sinusoidal distribution) as described by the following equations are investigated using the developed DQ formulation.

$$T(x,y) = \Delta T\,(x/a) \tag{31}$$

$$T(x,y) = \Delta T[1-(x/a)^2][1-(y/b)^2] \tag{32}$$

$$T(x,y) = \Delta T \sin(\pi x/a)\sin(\pi y/b) \tag{33}$$

The laminated plate is made of graphite/epoxy (AS-3501), whose material properties are presented in Table 1, with b/t=100 and cross-ply ratio of M=0.5. The results for critical temperature index ΔT_{cr} versus aspect ratio are shown in Figs. 7(a)-7(c), for the plate under linear, paraboloidal, and sinusoidal distributions, respectively. The results are presented for two types of edge support: SSSS and CCCC. Only the results of the simply supported plate are compared with those obtained by finite element analysis. The analysis is performed in ABAQUS using a four-node shell element, S4R5. The results for buckling mode shapes of plate with a/b=1 under sinusoidal thermal load for both types of edge supports are depicted in Fig. 8.

4.2 Parametric studies

In this section, the effects of several important parameters on the thermal buckling behavior of cross-ply laminated plates are investigated using the presented DQ formulation. In this parametric study, the laminate material and stacking sequence are assumed similar to those mentioned in Section 4.1.3 namely a [0°/90°/0°] symmetric cross-ply laminate made of graphite/epoxy (AS-3501). The plate has an aspect ratio of a/b=1.0, width to thickness ratio of b/t=100, cross-ply ratio of M=0.5, and edge support of the SSSS type, unless otherwise specified. The plate is subjected to the sinusoidal thermal load distribution given by Eq. (33). Some of the results are compared with those obtained by finite element analysis performed in ABAQUS.

Fig. 9 shows the effect of the thermal expansion coefficient ratio, α_2/α_1, on the plate critical temperature index, ΔT_{cr}. As the thermal expansion coefficient ratio increases from 0 to 1, the critical temperature index decreases by a rate similar to an exponential decay. This is a result of the increase in in-plane thermal forces. Consequently, the induced membrane forces increase.

Fig. 10 shows the effect of lamina stiffness ratio, E_1/E_2, on the plate critical temperature index, ΔT_{cr}. As the stiffness ratio increases, ΔT_{cr} increases by a nearly linear rate. This may be explained in this way that if E_1 increases and E_2 remains constant, cause an increase in the D_{11} stiffness. However, if E_2 decreases and E_1 remains constant, a decrease in thermal forces ensues, thereby resulting in decrease in mechanical force resultants. Therefore, we anticipate a rise in buckling load for both assumptions. This means that, to obtain a higher resistance to thermal buckling, a higher stiffness ratio should be considered. In Fig. 11, the effects of both aspect and stiff-

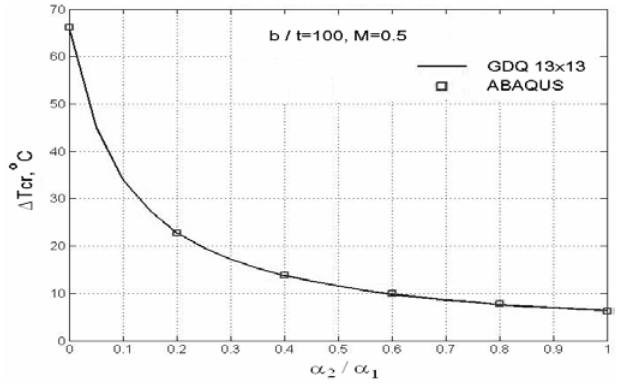

Fig. 9. Effect of thermal expansion coefficient ratio, α_2/α_1, on the critical temperature index, ΔT_{cr}, for a simply supported symmetric [0°/90°/0°] laminated plate (b/t=100, M=0.5).

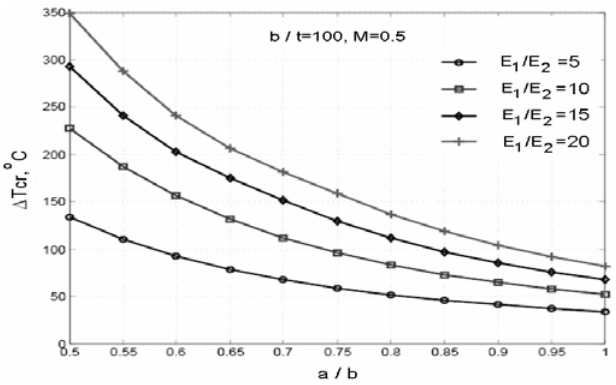

Fig. 11. Effect of aspect ratio and stiffness ratio on the critical temperature index, ΔT_{cr}, for a simply supported symmetric [0°/90°/0°] laminated plate (b/t=100, M=0.5).

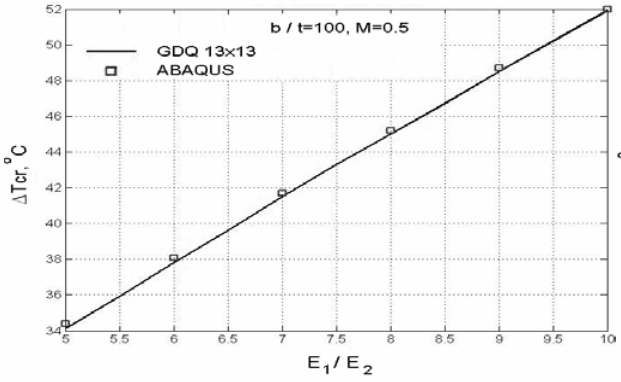

Fig. 10. Effect of stiffness ratio, E_1/E_2, on the critical temperature index, ΔT_{cr}, for a simply supported symmetric [0°/90°/0°] laminated plate (a/b=1, b/t=100, M=0.5).

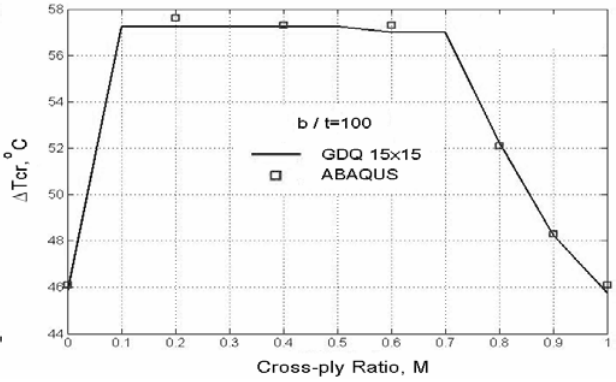

Fig. 12. Effect of the cross-ply ratio on the critical temperature index, ΔT_{cr}, for a simply supported symmetric [0°/90°/0°] lamin ated plate (a/b=1, b/t=100, M=0.5).

ness ratios on the plate thermal buckling temperature index, ΔT_{cr} are explored, and the results are shown as a curve set. For all values of E_1/E_2 as the aspect ratio increases from 0.5 to 1.0, ΔT_{cr} decreases. However, variations in a/b have lower effects in ΔT_{cr} as a/b approaches unity.

Finally, the effect of the cross-ply ratio, M, on the plate critical temperature index, ΔT_{cr} is depicted in Fig. 12. As M increases from 0 to approximately 0.1, ΔT_{cr} rises at a high slope. In the second interval, approximately from 0.1 to 0.7, the critical temperature remains constant, or has small variations. In the last interval, with M varying from approximately 0.7 to 1.0, the critical temperature rapidly declines. In Fig. 13, the effects of both aspect and cross-ply ratios on the plate buckling temperature index, ΔT_{cr}, are shown as a curve set.

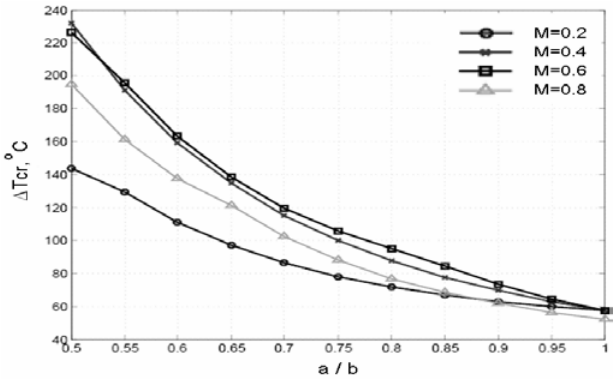

Fig. 13. Effect of aspect ratio and cross-ply ratio on the critical temperature index, ΔT_{cr}, for a simply supported symmetric [0°/90°/0°] laminated plate (b/t=100, M=0.5).

5. Concluding remarks

Thermal buckling induced by uniform or nonuniform temperature change in symmetric cross-ply laminated composite plates was studied using GDQM. The study reveals the following:

(1) The presented DQ formulation can accurately predict the thermal buckling behaviors of unidirectional and symmetric cross-ply laminates under uniform or non-uniform thermal loads.

(2) The presented differential quadrature model rapidly converges as the number of the grid points increases. For lower buckling modes, a set of 9×9 grid points, and for higher buckling modes, a set of 19×19 grid points, give accurate results.

(3) Unidirectionally laminated fibrous composite plates, restrained in the direction normal to fibers orientation, buckle in

higher mode shapes than the same laminates restrained along the fiber direction. Critical buckling temperature is not highly dependent on a/b, and approaches its constant minimum value at relatively low values of aspect ratio. This is in contrast with the behaviors of laminates restrained along the fiber direction.

(4) In symmetric cross-ply laminates, as the thermal expansion coefficient ratio, α_2/α_1, increases from 0 to 1, the critical temperature index decreases by a rate similar to an exponential decay.

(5) In symmetric cross-ply laminates, as the stiffness ratio, E_1/E_2, increases, the critical temperature index increases by an approximately linear rate.

(6) In symmetric cross-ply laminates, as cross-ply ratio increases from 0 to 1, ΔT_{cr} increases rapidly at a first subinterval. It then, remains with no considerable changes in an intermediate subinterval, and finally declines rapidly.

(7) Thermal buckling load is significantly influenced by temperature distribution and boundary conditions. Compared to simply supported plates, clamped plates are stiffer and their critical buckling temperatures are higher.

Nomenclature

A, B, D	:	Extensional, coupling, bending stiffness matrices
a, b, t	:	Length, width, thickness of plate
E_1, E_2	:	Lamina young's moduli in principal directions 1,2
G_{12}	:	Lamina shear modulus in principal plane 12
M_x, M_y, M_{xy}	:	Resultant mechanical moment components
M^T_x, M^T_y, M^T_{xy}	:	Resultant thermal moment components
N_x, N_y, N_{xy}	:	Resultant mechanical force components
N^T_x, N^T_y, N^T_{xy}	:	Resultant thermal force components
$[\bar{Q}]$	:	Transformed lamina stiffness matrix
$T(x,y)$	:	Temperature change
T_0	:	Temperature distribution index
u, v, w	:	Displacements along x, y, and z
X, Y, Z	:	Nondimensional Cartesian coordinates
x, y, z	:	Cartesian coordinates
α_x, α_y, α_{xy}	:	Transformed lamina thermal expansion coefficients
$\varepsilon^0_x, \varepsilon^0_y, \gamma^0_{xy}$	:	Midplane strains
$\kappa_x, \kappa_y, \kappa_{xy}$	:	Curvatures
ν_{12}, ν_{21}	:	Lamina Poisson's ratios in principal plane 12
$\sigma_x, \sigma_y, \tau_{xy}$	:	Stress components

References

[1] K. R. Thangaratnam and J. Ramachandran, Thermal Buckling of Composite Laminated Plates, *Comput. Struct*. 32 (1989) 1117–1124.

[2] L. W. Chen, E. J. Brunelle and L. Y. Chen, Thermal Buckling of Initially Stressed Thick Plates, *J. Mech. Des*. 104 (1982) 557–564.

[3] L. W. Chen and L. Y. Chen, Thermal Buckling of Laminated Cylindrical Plates, *Comput. Struct*. 8 (1987) 189–205.

[4] L. W. Chen and L. Y. Chen, Thermal Buckling Analysis of Composite Laminated Plates by the Finite Element Method, *J. Thermal Stresses*, 12 (1989) 41–56.

[5] W. J. Chen, P. D. Lin and L. W. Chen, Thermal Buckling Behavior of Thick Composite Laminated Plates Under Nonuniform Temperature Distribution, *Comput. Struct.* 41 (4) (1991) 637–645.

[6] R. M. Jones, Thermal Buckling of Uniformly Heated Unidirectional and Symmetric Cross-ply Laminated Fiber-Reinforced Composite Uni-axial in-Plane Restrained Simply Supported Rectangular Plates, *Composites Part A: Applied Science and Manufacturing*, 36 (2005) 1355–1367.

[7] S. P. Timoshenko and S. Woinowsky-Krieger, *Theory of Plates and Shells*, 2nd Ed., *McGraw-Hill*, New York, USA (1959).

[8] R. M. Jones, *Mechanics of Composite Materials*, *Tylor & Francis, Inc*. (1999).

[9] S. P. Timoshenko and J. N. Goodier, *Theory of Elasticity*, 3rd Ed., *McGraw-Hill*, New York, USA (1970).

[10] C. W. Bert and M. Malik, Differential Quadrature Method in Computational Mechanics: A Review, *Appl. Mech. Rev.* 49 (1) (1996).

M. M. Mohieddin Ghomshei received his M.Sc. in Mechanical Engineering from Sharif University of Technology, Iran, in 1992, and his Ph.D. from Tehran University, Iran, in 2002. Dr. Ghomshei is currently an Assistant Professor at the Department of Mechanical Engineering of Islamic Azad University-Karaj Branch in Iran. His research fields are mechanics of composite structures and smart materials and structures.